

Supporting Information for

New Insights into the Electrochemical Hydrogen Oxidation and Evolution Reaction Mechanism

J. Durst, A. Siebel, C. Simon, F. Hasché, J. Herranz, H. A. Gasteiger

Technische Universität München, Lehrstuhl für Technische Elektrochemie

Lichtenbergstr. 4, 85748 Garching (Germany)

E-mail: Julien.durst@tum.de

Homepage: <http://www.tec.ch.tum.de/>

I. Materials

Pt/C_{Vulcan} (5 wt.%, ref. TEC10V05E, Tanaka), Ir/C_{Vulcan} (20 wt.%, ref. P40A200, Premetek) and Pd/C_{Vulcan} (10 wt.%, ref. P30A100, Premetek) were used.

II. Electrochemical active surface area (ECSA) measurement

TEM observations of the catalysts were performed with a Jeol 2010 TEM operated at an accelerating voltage of 200 kV. Samples of TEM images for each catalyst are displayed from Figure S1 to Figure S3. Particle size distributions of the catalysts were reconstructed by measuring the diameter of at least 200 individual particles with the software ImageJ[®] from TEM images obtained at high magnifications, × 200 000 (Figure S4). For each particle size distribution the number-averaged diameter ($\overline{d_N}$) and the surface-averaged diameter ($\overline{d_S}$) were determined¹:

$$\overline{d_N} = \frac{\sum_{i=1}^n l_i d_i}{\sum_{i=1}^n l_i} \quad \text{Eq. S1}$$

$$\overline{d_S} = \frac{\sum_{i=1}^n l_i d_i^3}{\sum_{i=1}^n l_i d_i^2} \quad \text{Eq. S2}$$

l_i stands for the number of particles having a diameter (d_i). The number-averaged diameter ($\overline{d_N}$) is the mean mathematical diameter and the surface-averaged diameter ($\overline{d_S}$) the diameter reported to the average surface area of the particle. The surface-averaged diameter is the most relevant parameter in

electrocatalysis. This diameter is worth 2.6 nm, 3.9 nm and 2.9 nm for the Pt/C, Ir/C and Pd/C catalysts, respectively. The surface-averaged diameter can be converted in an electrochemical active surface area ($ECSA_{TEM}$, see Table 1 of the main manuscript) using the density (ρ) of each element:

$$ECSA_{TEM} = \frac{6}{\rho d_s} \quad \text{Eq. S3}$$

It yields to $ECSA_{TEM}$ values of 110, 68 and 173 $\text{m}^2 \text{g}^{-1}_{\text{metal}}$ for the Pt/C, Ir/C and Pd/C, respectively. ECSA values could be used by the reader to turn all surface normalized exchange current densities into mass normalized ones (for technical applications, exchange current densities reported in $\text{mA mg}^{-1}_{\text{metal}}$ are important).

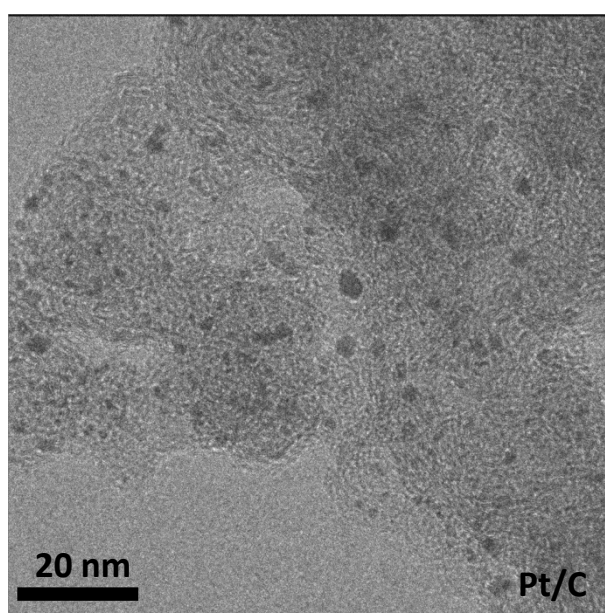


Figure S1. TEM image of the 5 wt.% Pt/C catalyst taken at 200 k magnification. The scale bar represents 20 nm.

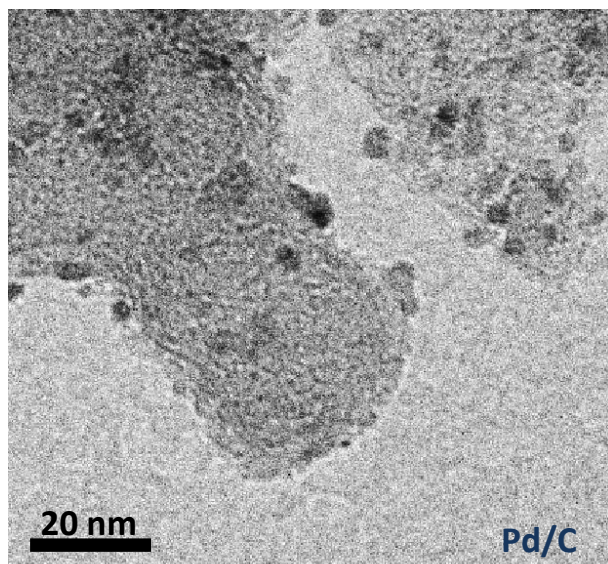


Figure S2. TEM image of the 10 wt.% Pd/C catalyst taken at 200 k magnification. The scale bar represents 20 nm.

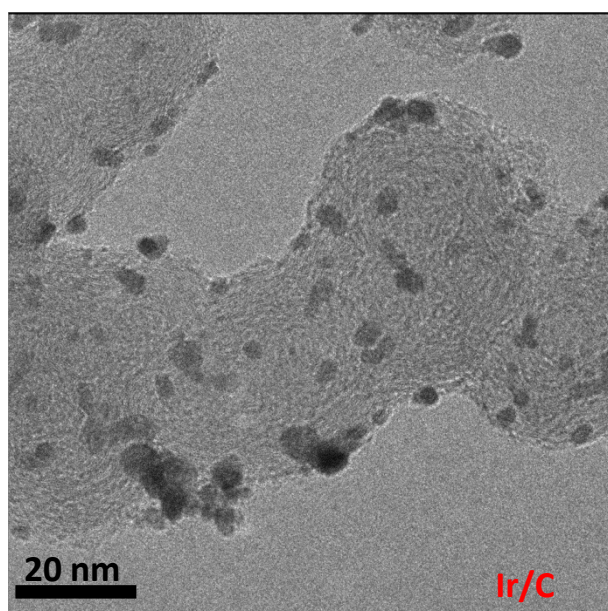


Figure S3. TEM image of the 20 wt.% Ir/C catalyst taken at 200 k magnification. The scale bar represents 20 nm.

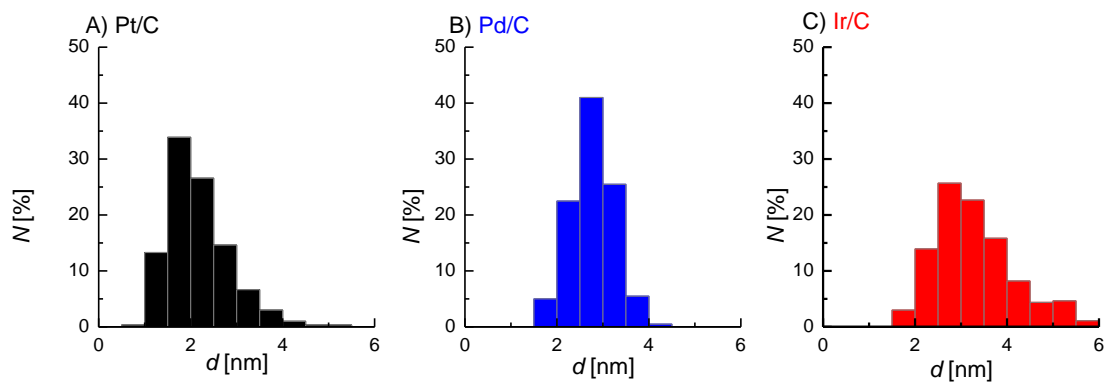


Figure S4. Particle size distribution of the A) 5 wt.% Pt/C, B) 10 wt.% Pd/C and C) 20 wt.% Ir/C catalysts, derived by counting at least 200 particles on TEM images taken at 200 k magnification.

To confirm the ECSA values found by TEM, this parameter was also measured using the H-UPD coulometry from the rotating disk electrode technique. The charges associated to the H-UPD process in acidic electrolytes (averaged over the adsorption and the desorption process, see the voltammograms reported in Figure 3) were turned into electrochemical active surface areas, $ECSA_{H-UPD}$, by using the reference charge densities ($210 \mu\text{C cm}^{-2}$ for Pt, $205 \mu\text{C cm}^{-2}$ for Pd² and $198 \mu\text{C cm}^{-2}$ for Ir³). The $ECSA_{H-UPD}$ values are $120 \pm 20 \text{ m}^2 \text{ g}^{-1}_{\text{Pt}}$ for the Pt/C catalyst, $105 \pm 20 \text{ m}^2 \text{ g}^{-1}_{\text{Pd}}$ for the Pd/C catalyst and $59 \pm 9 \text{ m}^2 \text{ g}^{-1}_{\text{Ir}}$ for the Ir/C catalyst. These values are in reasonable agreement with the ones determined by TEM (110 , 173 , and $68 \text{ m}^2 \text{ g}^{-1}_{\text{metal}}$ for the Pt/C, Pd/C, and Ir/C, respectively).

III. PEMFC measurements

5 cm^2 MEAs were prepared by the decal transfer method. The working electrode loadings, deduced from the weights of the decals before and after hot-pressing, were roughly estimated to be 3, 8, and $16 \mu\text{g}_{\text{metal}} \text{ cm}^{-2}_{\text{geo}}$ for the Pt/C, Ir/C, and Pd/C catalysts, respectively. The counter/reference electrode was made of a 50 wt.% Pt/C catalyst ($0.3 \text{ mg}_{\text{Pt}} \text{ cm}^{-2}_{\text{geo}}$ using TEC10V50E, Tanaka). The membrane was a Nafion XL[®] with a $30 \mu\text{m}$ thickness. All other parameters are identical to those reported by Neyerlin and co-workers.⁴ HOR/HER kinetics were recorded with the anode inlet flushed with 200 nccm fully humidified H₂ and the anode outlet connected to the cathode inlet. Additionally, voltammograms were recorded at 100 mV s^{-1} with the working electrode/cathode flushed with 5 nccm humidified N₂ and the reference-counter electrode/anode flushed with 50 nccm humidified diluted 5% H₂ in N₂.

IV. RDE measurements

A PTFE jacketed cell was used in a three electrode configuration (Pt as counter and Ag/AgCl as reference electrodes). The electrolyte solution was freshly prepared with NaOH×H₂O (99.9995 %, Fluka) and ultrapure water. All potentials were converted into and are reported versus the reversible hydrogen electrode (RHE) scale. The catalyst loadings on the polished 0.196 cm² glassy carbon disk were 2.5 μg_{Pt} cm⁻²_{geo} for the Pt/C catalyst and 5 μg_{metal} cm⁻²_{geo} for the Pd/C and Ir/C catalysts (adjusted by depositing a 10 μL aliquot of an ink). After electrochemical cleaning at 100 mV s⁻¹ under argon at 293 K between 0.05 and 1.00 V_{RHE} until steady state voltammograms were obtained, the cell was heated to 313 K and purged with H₂ (6.0; Westfalen AG) for 15 min.

There are two important parameters to consider when preparing a rotating disk electrode: the metal and the carbon loading. In the case of the carbon loading, although it does not play direct a role on the HOR/HER kinetics, its loading determines the electrode layer thickness. Working with thick electrode films could induce severe mass transport issues which could in turn hinder the determination of some kinetic parameters. In this study, we aimed at comparing the same materials in H₂-pump/PEMFC and RDE, and the choice of the materials have been done according to the principle of the H₂-pump/PEMFC method (see Neyerlin et al.⁴, who pointed out the importance of using low metal loadings on carbon). Therefore, with these low weight ratios of metal onto carbon, only small metal loading were used in this study in order not to have carbon loadings higher than 50 μg_C cm⁻²_{geo}. Having this in mind, Pt/C Ir/C and Pd/C electrodes were then prepared with similar metal loadings with reasonably small carbon loadings. The low metal loading combined with the lower HOR/HER activity of iridium and its early onset of oxide formation is the reason why the diffusion limited current density was not reached for the Ir/C catalyst shown in Fig. 1B.

V. HOR polarization curves

Same conditions ($T=313$ K, H₂-saturated atmosphere and ambient pressure) were used in PEMFC and RDE. Polarization curves were recorded by sweeping the potential of the working electrode at 10 mV s⁻¹ for RDE measurements (2 mV s⁻¹ for PEMFC measurements) between -0.1 and +1.0 V_{RHE} at 1600 rpm (rotation per minute). 5 cycles were recorded and data were obtained from the last, negative going scan. Potentials were corrected for ohmic losses, measured by impedance spectroscopy before and after each polarization curve ($R_{\text{HFR}} \approx 0.1 \Omega \text{ cm}^2$ for PEMFC measurements and $\approx 50 \Omega$ for RDE measurements). Extraction of the kinetic currents from RDE measurements is detailed below. For surface area normalization in RDE, since the loadings are well defined and owing to the less well defined H-UPD features in base, cm²_{metal} were determined from the loading and the H-UPD areas measured in 0.1 M HClO₄ (Pt/C and Pd/C) or 0.05 M H₂SO₄ (Ir/C). For surface area normalization in PEMFC, since the very low working electrode loadings are difficult to determine by weight

measurements (<1 mg_{catalyst} on a 5 cm² electrode), the cm²_{metal} was determined from the well-defined H-UPD process measured in PEMFC (reported in Fig. S5).

VI. Extraction of the exchange current densities (i^0)

For RDE measurements, kinetic currents (i_{kin}) were extracted from the raw polarization plots by considering the limited current densities (i_{lim}) and current (i) achieved at 1600 rotation per minute:

$$i_{\text{kin}} = \frac{i \times i_{\text{lim}}}{i_{\text{lim}} - i} \quad \text{Eq. S4}$$

At this point, only kinetic currents up to 80 % of i_{lim} were considered.⁵ For surface area normalization (from A cm⁻²_{geo} to A cm⁻²_{metal}) in RDE, since the electrode loadings are well defined and owing to the less well defined H-UPD features in base, cm²_{metal} were determined from the loading and the H-UPD areas measured in 0.1 M HClO₄ (Pt/C and Pd/C) or 0.05 M H₂SO₄ (Ir/C). For surface area normalization in PEMFC, since the working electrode loading are difficult to determine by weight measurements (<1 mg_{catalyst} on a 5 cm² electrode), the cm²_{metal} was determined from the well-defined H-UPD (see the CV reported in Fig. S5).

PEMFC and RDE polarization curves were then fitted to a Butler-Volmer regime (described in the manuscript; see gray lines in the upper part of Fig. 2):

$$i = i_{313\text{K}}^0 \times \left(e^{\frac{\alpha F \eta}{RT}} - e^{-\frac{(1-\alpha) F \eta}{RT}} \right) \quad \text{Eq. S5}$$

Exchange current densities ($i_{313\text{K}}^0$) are reported in Table S1-S3. Additionally, the micro-polarization regions, from -10 mV to +10 mV, were also fitted with the following equation and the corresponding exchange current densities are also reported in Table S1-S3:

$$i_{313\text{K}}^0 = \frac{i RT}{\eta F} \quad \text{Eq. S6}$$

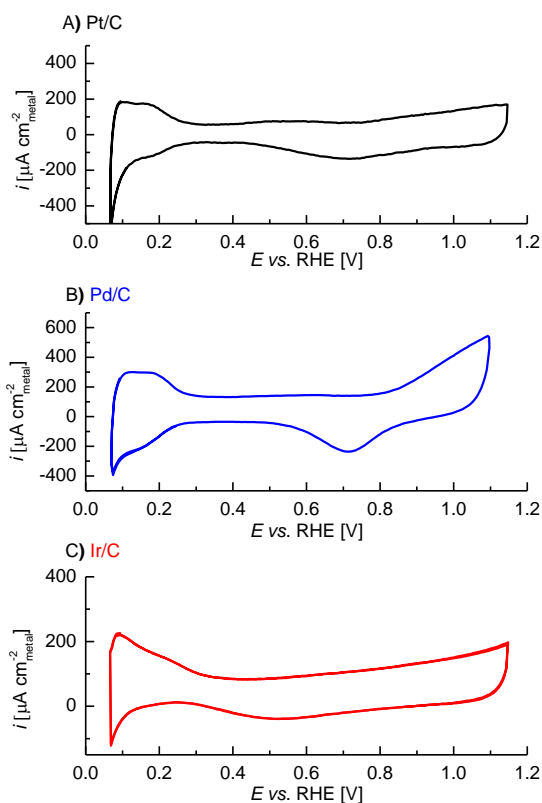


Figure S5. Cyclic voltammograms recorded in 5 cm^2 active area PEMFC for the Pt/C (in black line), the Pd/C (in blue line) and the Ir/C (in red line) catalysts at 100 mV s^{-1} , room temperature, and ambient gas pressure. The loadings of the working electrode were 3 , 16 , and $8 \mu\text{g}_{\text{metal}} \text{ cm}^{-2}$ for the Pt/C, Pd/C, and Ir/C catalysts, respectively. Surface normalization was performed using the H-UPD coulometry, and a charge density of *ca.* $210 \mu\text{C cm}^{-2}$ for Pt/C, $205 \mu\text{C cm}^{-2}$ for Pd², and $198 \mu\text{C cm}^{-2}$ for Ir/C³. The working electrode/cathode was flushed with 5 nccm humidified N_2 . The reference-counter electrode/anode was flushed with 50 nccm humidified $5\% \text{ H}_2$ in N_2 (in order to reduce the H_2 -crossover).

Table S1. HOR/HER exchange current densities (i_{313K}^0) measured in PEMFC and 0.1 M NaOH electrolyte setup at 313 K and $p_{H_2} \approx 100$ kPa_{abs} determined from a fit of the Butler-Volmer equation (Eq. 6) and the micropolarization equation (Eq. 7) for the Pt/C catalyst. Values are reported for a series of three measurements in 0.1 M NaOH electrolyte solution and two measurements in PEMFC. For each media, the Butler-Volmer and micropolarization extracted exchange current densities are averaged into one unique value. The error bar is the standard deviation between all these values. Best fits of the Butler-Volmer equation were obtained with α -values of 0.52 ± 0.06 in PEMFC and 0.38 ± 0.08 in RDE. In the work of Sheng et al.⁶, the HOR/HER kinetics were fitted with a fixed value of $\alpha = 0.5$ in the Butler Volmer equation, although it can be seen in the figures shown by Sheng et al that the HOR branches were less steep than the fits, suggesting slightly lower α parameters for the HOR branch, as are found in the present study.

catalyst	media, fitting method	i_{313K}^0 [mA cm ⁻² _{metal}]			
		#1	#2	#3	average
Pt/C	0.1M NaOH, Butler-Volmer	1.5	1.2	1.1	1.0±0.1
	0.1M NaOH, micropolarization	0.9	0.8	0.8	
	PEMFC, Butler-Volmer	249	162	---	216±50
	PEMFC, micropolarization	269	185	---	

Table S2. HOR/HER exchange current densities (i_{313K}^0) measured in PEMFC and 0.1 M NaOH electrolyte setup at 313 K and $p_{H_2} \approx 100$ kPa_{abs} determined from a fit of the Butler-Volmer equation (Eq. 6) and the micropolarization equation (Eq. 7) for the Pd/C catalyst. Values are reported for a series of three measurements in 0.1 M NaOH electrolyte solution and two measurements in PEMFC. For each media, the Butler-Volmer and micropolarization extracted exchange current densities are averaged into one unique value. The error bar is the standard deviation between all these values. Best fits of the Butler-Volmer equation were obtained with α -values of 0.35 ± 0.1 in PEMFC and 0.43 ± 0.07 in RDE.

catalyst	media, fitting method	i_{313K}^0 [mA cm ⁻² _{metal}]			
		#1	#2	#3	average
Pd/C	0.1M NaOH, Butler-Volmer	0.06	0.04	0.07	0.06±0.02
	0.1M NaOH, micropolarization	0.08	0.04	0.09	
	PEMFC, Butler-Volmer	6.4	3.2	---	5.2±1.2
	PEMFC, micropolarization	6.0	5.2	---	

Table S3. HOR/HER exchange current densities (i_{313K}^0) measured in PEMFC and 0.1 M NaOH electrolyte setup at 313 K and $p_{H_2} \approx 100 \text{ kPa}_{\text{abs}}$ determined from a fit of the Butler-Volmer equation (Eq. 6) and the micropolarization equation (Eq. 7) for the Ir/C catalyst. Values are reported for a series of three measurements in 0.1 M NaOH electrolyte solution and two measurements in PEMFC. For each media, the Butler-Volmer and micropolarization extracted exchange current densities are averaged into one unique value. The error bar is the standard deviation between all these values. Best fits of the Butler-Volmer equation were obtained with α -values of 0.51 ± 0.01 in PEMFC and 0.48 ± 0.02 in RDE.

catalyst	media, fitting method	$i_{313K}^0 [\text{mA cm}^{-2}_{\text{metal}}]$			
		#1	#2	#3	average
Ir/C	0.1M NaOH, Butler-Volmer	0.29	0.52	0.27	0.37±0.12
	0.1M NaOH, micropolarization	0.31	0.54	0.30	
	PEMFC, Butler-Volmer	35	53	---	45±8
	PEMFC, micropolarization	39	54	---	

References

1. S. Trasatti and O. A. Petrii, *J. Electroanal. Chem.*, 1992, 327, 353-376.
2. M. Hara, U. Linke and T. Wandlowski, *Electrochim. Acta*, 2007, 52, 5733-5748.
3. T. Pauporté, F. Andolfatto and R. Durand, *Electrochim. Acta*, 1999, 45, 431-439.
4. K. C. Neyerlin, W. Gu, J. Jorne and H. A. Gasteiger, *J. Electrochem. Soc.*, 2007, 154, B631-B635.
5. P. Rheinländer, S. Henning, J. Herranz and H. A. Gasteiger, *ECS Trans.*, 2013, 50, 2163-2174.
6. W. Sheng, H. A. Gasteiger and Y. Shao-Horn, *J. Electrochem. Soc.*, 2010, 157, B1529-B1536.